Synthesis and photocatalytic performances of Al and Ce co-doped ZnO powders

SHI FENG NIU[a], RUN MEI ZHANG[b], JIA HONG ZHENG[b,c*]
[a]*Key Laboratory Automotive Transportaion Safety Technology Ministry of Communication, Chang'an University, Xi'an, 710064, P. R. China*
[b]*School of Materials Science and Engineering, Chang'an University, Xi'an 710064, P. R. China*
[c]*Key Laboratory of Preparation and Applications of Environmental Friendly Materials, Ministry of Education, Jilin Normal University, Siping 136000, P. R. China*

($Zn0_{.97-x}Ce_{0.03}Al_xO$, x=0.00, 0.02, 0.04, 0.06, 0.08, 0.10) powders have been prepared by a sol-gel method, and their structural, morphology and photocatalytic activities have been investigated. The obtained powders analyses by different techniques such as X-ray diffraction (XRD), scanning electron microscopy (SEM) and ultra-violet visible spectroscopy (UV–Vis.). Their photodegradation efficiencies for methylene blue and rhodamine B dye aqueous solutions under Xenon lamp light irradiation were investigated in detail. The results show that with the increase concentration of the main group metal Al, photocatalytic activity of Al and Ce co-doped ZnO was increased, and the total degradation rate is close to a function distribution with time, the photocatalytic reaction occurs rapidly and obviously it is the good photocatalytic material.

(Received December 25, 2016; accepted April 5, 2018)

Keywords: Al and Ce co-doped ZnO, Sol-gel, Photocatalytic activities

1. Introduction

The increase in the use of organic pollutants in various industries nowadays becomes a major source of environmental contamination. Wastewater treatment and recycling are an important concern, and the researchers are looking forward for inexpensive and suitable technologies. Hence, pollution treatment should be a major concern [1]. One of the best and green environmentally friendly ways to reduce contamination of water is photocatalysis. The heterogeneous photocatalysis has attracted much attention as a 'green' technique [2-5]. The photocatalytic activity of catalyst has been correlated with electronic, structural and morphological properties i.e., band gap energy, crystalline structure, surface area and particle size. In view of diverse applications of photocatalysts, researchers are trying to control these properties for efficient photocatalytic activity [6-7]. In the last two decades, photocatalys is in the presence of semiconductors caused a wide range of concern because it can be used in environmental protection [8-12]. Semiconducting oxide photocatalysts have received increased attention for the degradation of inorganic and organic pollutants [13]. The most frequently used photocatalyst is TiO_2, but in recent years ZnO is found to be a suitable alternative to TiO_2 due to its similar band gap energy, high photosensitivity, non-toxic nature, low cost and chemical stability [14]. Zinc oxide provides physicochemical properties that could lead to numerous applications in the field of photocatalysis [15]. Previous studies [5] have shown the photocatalytic activities of ZnO for the degradation of a wide range of pollutants.

Recently, adding impurities into a wide gap semiconductor such as ZnO induces great changes in the optical, electrical and magnetic properties [16]. Thus doping of semiconductors with certain elements offers an effective approach to adjust their properties which is crucial for their practical applications. To control the properties of ZnO nanostructures several doping elements have been used [17]. Doping ZnO with selective elements, e.g., noble metals [18], transition metal oxides [19], rare-earth metals [20] and main-group metal oxides [21], has been considered as effective methods to modify optical, magnetic, electrical and gas-sensing properties of semiconductor materials.

It is known that metal ion doping can modify the surface properties of ZnO, hinder the recombination of photogenerated electron-hole pairs and increase the amount of the active sites. Among them, Al-doped ZnO has also received considerable attention because of its unique physico-chemical properties as well as the merit of cheap raw materials [22]. Especially, Al-doped ZnO is potential candidate for the practical application in adsorption of organic compounds [22]. Nowadays rare earth ion doped semiconductors have become more popular among researchers because of their unique optical properties and promising applications in optoelectronic devices [17–19]. Photocatalytic activity of ZnO can be significantly enhanced by doping with the lanthanide ions having 4f configuration [14]. Among them, cerium doping has attracted more interest due to comparatively large ion which produces a localized charge perturbation during

substitutional doping into ZnO lattice and increases its photocatalytic activity.

Due to photocatalytic process mainly occurs on surface of ZnO photocatalysts, powder ZnO which have large specific surface area were utilized in wastewater treatment usually [12, 23]. In the present work, Al and Ce co-doped ZnO nano-powders were successfully synthesized by sol-gel method at room temperature. The effects of co-doping elements on ZnO and nanocrystals are investigated by study of structural, morphological, and photocatalytic activities using methylene orange, and rhodamine B solution as the target degradation under Xenon lamp light.

1.1. Experimental

The chemical reagents $Zn(NO_3)_2{\cdot}6H_2O$, $Al(NO_3)_2{\cdot}6H_2O$, and $C_6H_8O_7{\cdot}H_2O$, $Ce(NO_3)_3{\cdot}12H_2O$ used in the experiment were all analytical reagent. The aqueous solution of zinc nitrate (0.1 M $Zn(NO_3)_2{\cdot}6H_2O$), aluminum nitrate (0.1 M $Al(NO_3)_2{\cdot}6H_2O$), cerium nitrate (0.1 M $Ce(NO_3)_3{\cdot}12H_2O$) and citric acid (0.3 M $C_6H_8O_7{\cdot}H_2O$). After 30 minutes magnetic stirring of the four solutions and quantitative cerium solution, the $Zn(NO_3)_2{\cdot}6H_2O$ and $Al(NO_3)_2{\cdot}6H_2O$ were mixed in different proportions $Zn_{0.97-x}Ce_{0.03}Al_xO$ (x=0.00, 0.02, 0.04, 0.06, 0.08, 0.10). Then blended the above mixed solution with the same amount of $C_6H_8O_7{\cdot}H_2O$, magnetic stirring for 3 hours to form sol. The sol was placed in a 80 ℃ drying oven for a certain period to form a dry gel. The dried gel was performed in an oven at 130 ℃ for long enough time, and the precursor was obtained by dehydration and expansion. The precursor was annealed at 400 ℃ for 2h.

1.2. Characterization

The crystalline analysis of $Zn_{0.97-x}Ce_{0.03}Al_xO$ was performed at room temperature using X-ray diffraction (XRD) (Bruker, D8 Advance, Germany) with an incident X-ray beam with Cu Kα at 1.5406 Å radiations. The morphologies of samples were observed by scanning electron microscope (SEM) (Hitachi, S-570, Japan). UV absorption spectra were obtained using double beam ultra-violet visible (UV–Vis.) spectrophotometer (Lengguang, 1901PC, China).

2. Results and discussion

2.1. Structure analysis

The crystalline phase and structure of the different Al and Ce co-doped ZnO ($Zn_{0.97-x}Ce_{0.03}Al_xO$, x=0.00, 0.02, 0.04, 0.06, 0.08, 0.10) microstructure are studied by XRD analysis. As shown in Fig. 1, all of the identified peaks in the XRD pattern can be attributed to the wurtzite phase ZnO (JCPDS no. 36-1451), indicating that ZnO have a wurtzite structure. No additional peaks corresponding to impurity phases (arising from Ce or/ and Al elements or related oxides) can be detected within the resolution of the X-ray diffractometer, which shows that the Al and Ce co-doping ZnO formation of single pure ZnO phase. As can be seen in the patterns, the diffraction peaks correspond to the (100), (002), (101), (110), (103), (200), (112), (201). This conforms that the structure of the doped ZnO retains the wurtzite phase belonging to the space group $P6_3mc$. This indicates the complete dissolution of Al^{3+} and Ce^{3+} within ZnO crystal lattice by occupying Zn^{2+} sites, which has no effect in the complete crystal structure of ZnO. It can be noticed that (101) peak of all the co-doped samples is found to be the most intense, which means that grain growth occurs priority along (101) plane. This is in good agreement with some previous results reported in the literature, such as Al-doped ZnO [24] and Ce-doped ZnO [25].

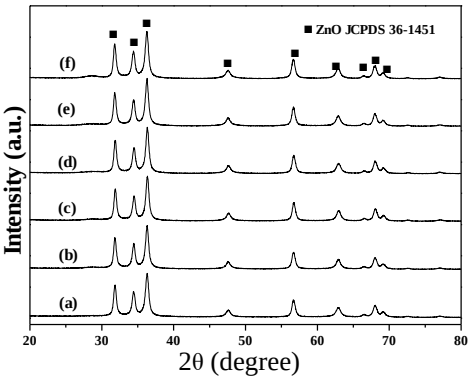

Fig. 1. XRD pattern of Al and Ce co-doped ZnO powders for different doping concentratin (a) (0% Al, 3 % Ce), (b) (2 % Al, 3 % Ce), (c) (4 % Al, 3 % Ce), (d) (6 % Al, 3 % Ce), (e) (8 % Al, 3 % Ce), (f) (10 % Al, 3 % Ce)

2.2. Morphology analysis

The surface morphologies of Al and Ce co-doped ZnO powders for different doping concentratin ($Zn_{0.97-x}Ce_{0.03}Al_xO$, x=0.00, 0.02, 0.04, 0.06, 0.08, 0.10) powders were confirmed using SEM analysis, the corresponding images are shown in Fig. 2. It can been see from the Fig. 2 (a) that the ZnO sample with single doped Ce consists of a large number of loose particles, but the particles size is about 50-100 nm are uniform and have good dispersion performances. Fig. 2 (b) is the 2% Al and 3% Ce co-doped ZnO SEM image, the particles are connected form a skeleton structure. Fig. 2(c) is the 4% Al and 3% Ce co-doped ZnO SEM image, the sample surface has rough slightly larger pores but with a stronger sense of hierarchy, which is similar to the layered rock profile. Fig. 2(d) is the 6% Al and 3% Ce co-doped ZnO, the structure is very dense with long strips of each other to bond to the growth, also, there are also many holes in the structure. Fig. 2(e) is the SEM photo of 8% Al and 3% Ce co-doped ZnO, the overall accumulation of the shape is a strip or long, the surface is rough but dense bulk, the

majority of the area is connected to the network. Fig. 2 (f) is 10% Al and 3% Ce co-doped ZnO, the network structure is composed of many small particles, and like sponges. Therefore, Al and Ce co-doping have some influence on the morphology of ZnO, but the influence is not very large, which is consistent with the XRD results.

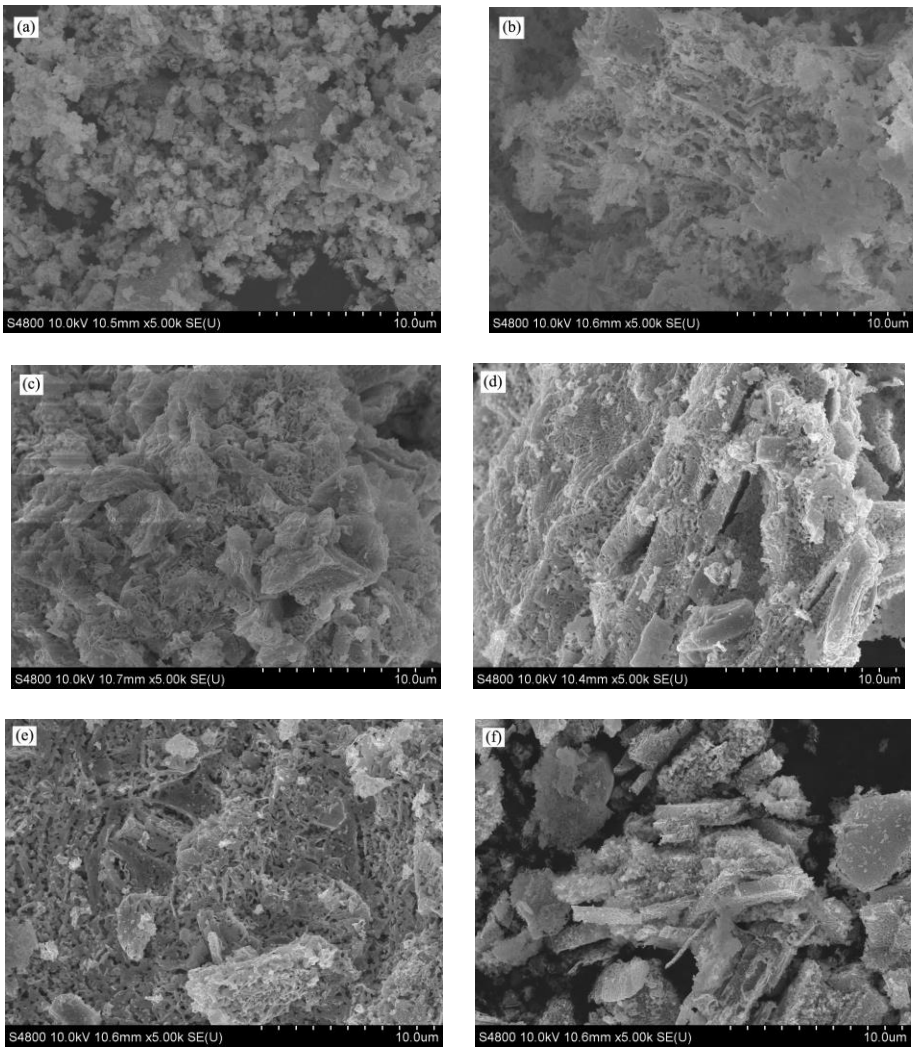

Fig. 2. FESEM images of the Al and Ce co-doped ZnO powders for different doping concentratin (a) (0% Al, 3 % Ce), (b) (2 % Al, 3 % Ce), (c) (4 % Al, 3 % Ce), (d) (6 % Al, 3 % Ce), (e) (8 % Al, 3 % Ce), (f) (10 % Al, 3 % Ce)

2.3. Photocatalytic analysis

To evaluate the photocatalytic activities of the synthesized photocatalysts, organic dye methylene blue, rhodamine B were selected as a model pollutant and the photodegradation of methylene blue, rhodamine B was studied over all the as-prepared $Zn_{0.97-x}Ce_{0.03}Al_xO$ powders for different doping concentratin samples, respectively. The photocatalytic decomposition of methylene blue, rhodamine B was carried out in a beaker containing a suspension of 20 mg $Zn_{0.97-x}Ce_{0.03}Al_xO$ powders for different doping concentratin in 20 mL of methylene blue, rhodamine B aqueous solution (20 mg/L) under Xenon lamp with an UV cut off filter was used as the visible light irradiation source, respectively. The reaction system was stirred for 30 min in the dark to reach the adsorption-desorption equilibrium before the irradiation. The UV-Vis absorption spectra of all the samples which were taken as the time changed were tested at room temperature. Fig. 3 displays schematic diagram of the experimental device for photocatalytic reaction.

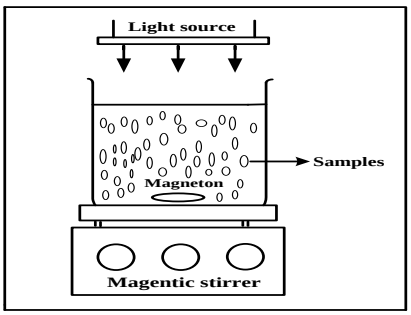

Fig. 3. Schematic diagram of the experimental device for photocatalytic reaction

To measure how much of methylene blue and rhodamine B were degraded, UV–Vis spectrophotometer was used, which analyzed maximum absorption (MA) level at 664 nm and 554 nm, corresponding to its wavelength of maximum absorption, these percentages of material degradation efficiency were utilized as response surface according to the statistical design study. Fig. 4 displays methylene blue molecular structure. Fig. 5 displays rhodamine B molecular structure.

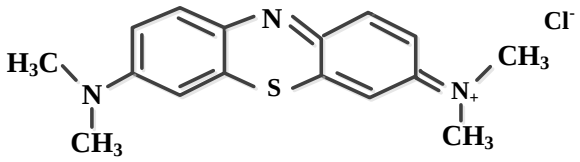

Fig. 4. Methylene blue molecular structure

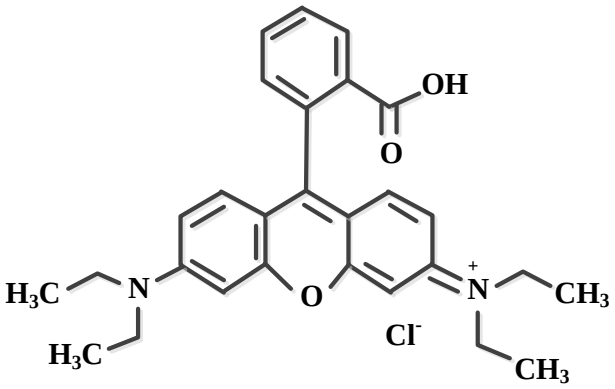

Fig. 5. Rhodamine B molecular structure

The effect of methylene blue and rhodamine B photodegradation by Al and Ce co-doped ZnO powders for different doping concentratin is illustrated by the variation of $(A_0–A_t)/A_0$ ratio as function of exposure time (where A_0 is the initial absorbance of methylene blue after stirring for 30 min in the dark and rhodamine B and A_t is the absorbance at time t). A remarkable degradation of methylene blue and rhodamine B with exposure time can be observed, resulting in the discoloration of the solution. The degradation rate is calculated using the following formula [24]:

$$\text{Degradation rate}=\frac{A_0-A_t}{A_0}\times 100\ \% \qquad (1)$$

In preliminary experiments conducted in the absence of the photocatalyst, no significant photolysis of the dye was observed during 120 min of irradiation. Once the catalyst added, the photodegradation was monitored by the time dependent UV–visible spectral changes of methylene blue and rhodamine B in the presence of Al and Ce co-doped ZnO powders for different doping concentratin (Fig. 6) and (Fig. 7).

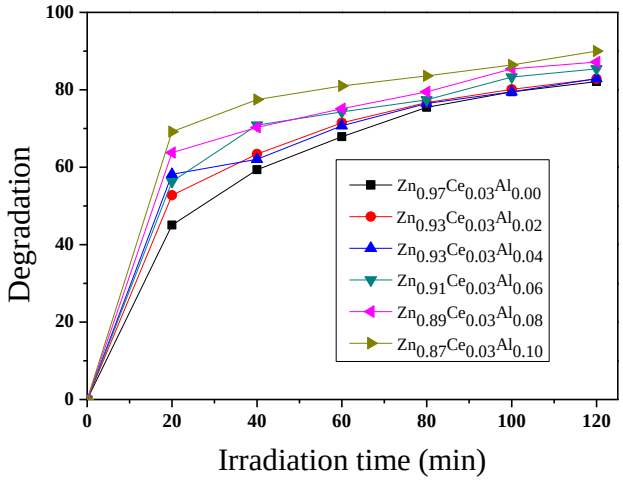

Fig. 6. Degradation rate of methylene blue under irradiation at wavelength of 664 nm in the presence of Al and Ce co-doped ZnO powders for different doping concentratin for different exposure times

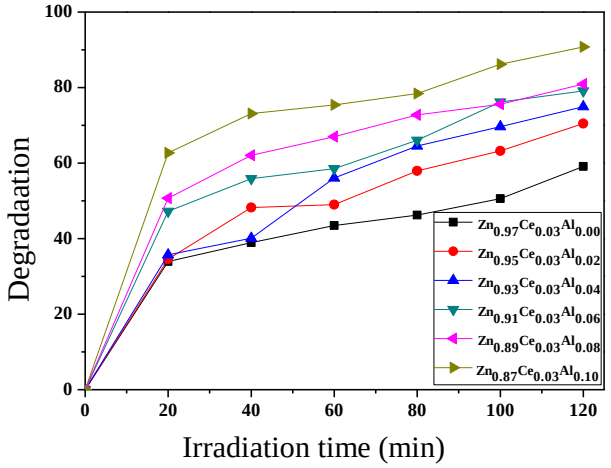

Fig. 7. Degradation rate of rhodamine B under irradiation at wavelength of 554 nm in the presence of Al and Ce co-doped ZnO powders for different doping concentratin for different exposure times

It can be clearly seen that from the Fig. 6 and Fig. 7 with the increase of Al^{3+} content, the photocatalytic rate of ZnO samples has been very significantly enhanced, especially in the case of $Zn_{0.87}Ce_{0.03}Al_{0.10}O$ almost just a photocatalytic efficiency reached more than 95%, and the overall degradation rate with time change graph is close to a straight line. In addition, it is obvious that photocatalyst under the same conditions has a better degradation rate of methyl blue than rhodamine B. The slope of the overall photocatalytic rate with time is very large, the photocatalytic reaction is rapid and obvious. And with the increase of Al^{3+} content, there is no downward trend, so the amount of Al^{3+} is not reached saturation. It can guess if Al^{3+} volume continues to improve, there's hope for further improvement of photocatalytic rate. So Al and Ce doped ZnO nanopowders photocatalytic materials are ideal.

The possible mechanism of photocatalytic degradation of methylene blue and rhodamine B dye can be understood as follows. Doping induces modifications in the electronic band structure of photocatalysts. These electronic changes remove the limitation of confined usage of photocatalysts in Xenon lamp light irradiation. Upon visible light irradiation, electrons (e^-) are excited from the valence band of ZnO to its conduction band, leaving the corresponding holes (h^+) in the valence band. Since the conduction band of ZnO is higher in energy than the new equilibrium Fermi energy level of Al and Ce co-doped ZnO, the photoexcited electrons on the conduction band are transferred from ZnO to doping elements [28].

$$\mathrm{ZnO}+h\nu \rightarrow \mathrm{ZnO}(e^-_{\mathrm{BC}}+h^+_{\mathrm{BV}}) \quad (2)$$

The photo-induced electrons are easily trapped by electronic acceptors such as adsorbed O_2 to produce a superoxide anion radical $\cdot O_2^-$:

The photo-induced holes are easily trapped by negative species OH^- hence favouring the production of hydroxyl radical species $\cdot OH$:

$$\mathrm{ZnO}(h^+_{\mathrm{BV}})+\mathrm{OH}^- \rightarrow \cdot\mathrm{OH} \quad (3)$$

These processes effectively suppress the electron–hole recombination and produce excess free radicals necessary for the degradation of methylene blue and rhodamine B.

$$\text{Rhodamine B}+\cdot O_2^- \text{ or } \cdot OH \rightarrow \text{decomposed products} \rightarrow CO_2+H_2O \quad (4)$$

$$\text{Methylene blue}+\cdot O_2^- \text{ or } \cdot OH \rightarrow \text{decomposed products} \rightarrow CO_2+H_2O \quad (5)$$

The active oxygen species and hydroxyl radicals react with methylene blue and rhodamine B to form decomposed products, which the finally products are CO_2 and H_2O. Therefore, the photocatalytic activity of Al and Ce co-doped ZnO is greatly improved.

3. Conclusions

In summary, Al and Ce co-doped ZnO powders with different Al doping concentration were prepared by sol-gel method. XRD analysis confirms the formation of single hexagonal ZnO wurtzite phase with high crystallinity. SEM observations reveal that the morphology of the samples is affected by the doping concentration. The sample of sponge morphology is beneficial to the adsorption capacity of organic dyes. Al and Ce co-doped ZnO powders show relative high photocatalytic activity for degradation methylene blue and rhodamine B dye under Xenon lamp light irradiation. The photocatalytic activity of methylene blue and rhodamine B dye exhibits a degradation rate around 90 % and 90 %, which is achieved for the duration of 120 min for Al and Ce co-doped ZnO powders. Therefore, the results can promote the potential application of ZnO in the field of water purification, gas sensing, dye sensitized solar cells etc.

Acknowledgements

The work was funded by the National Natural Science Foundation of China (Grant nos. 21607013 and 51602026), and the Special Fund for Basic Scientific Research of Central Colleges, Chang'an University (300102318108, 300102228202, 300102318402). Authors are thank full to the supports.

References

[1] C. Zhang, Y. F. Zhu, Chem. Mater. **17**, 3537 (2005).
[2] R. Saravanan, V. K. Gupta, E. Mosquera, F. Gracia, M. M. Khan, V. Narayanan, A. Stephen, RSC Adv. **5**, 34645 (2015).
[3] R. Saravanan, V. K. Gupta, E. Mosquera, F. Gracia, M. M. Khan, V. Narayanan, A. Stephen, J. Col. Interf. Sci. **452**, 126 (2015).
[4] A. Elaziouti, N. Laouedj, A. Bekka, Environ. Sci. Pollut. Res. **23**, 15862 (2016).
[5] E. Abdelkader, L. Nadjia, B. Naceur, B. Noureddine, J. Alloys Compd. **679**, 408 (2016).
[6] L. Hu, S. Dong, Q. Li, Y. Li, Y. Pi, M. Liu, X. Han, J. Sun, J. Alloys Compd. **649**, 400 (2015).
[7] G. S. Zhang, M. N. Nadagouda, K. O'Shea, S. M. El-Sheikh, A. A. Ismail, V. Likodimos, P. Falaras, D. D. Dionysiou, Catal. Today **224**, 49 (2014).
[8] C. Pan, R. Ding, Y. C. Hu, G. J. Yang, Physica E **54**, 138 (2013).
[9] J. Tripathy, K. Y. Lee, P. Schmuki, Angew. Chem. Int. Ed. **53**, 12605 (2014).
[10] S. M. Jilani, P. Banerji, ACS Appl. Mater. Interfaces **6**, 16941 (2014).
[11] F. Jamali-Sheini, R. Yousefi, N. A. Bakr, M. Cheraghizade, M. Sookhakian, N. M. Huang, Mater. Sci. Semicond. Process. **32**, 172 (2015).
[12] J. Wang, J. H. Yang, X. Y. Li, D. D. Wang, B. Wei, H. Song, X. F. Li, S. W. Fu, Physica E **75**, 66 (2016).
[13] C. Zhang, Y. F. Zhu, Chem. Mater. **17**, 3537 (2005).
[14] R. Saravanan, V. K. Gupta, E. Mosquera, F. Gracia, M. M. Khan, V. Narayanan, A. Stephen, RSC Adv. **5**, 34645 (2015).
[15] R. Slama, J. El Ghoul, I. Ghiloufi, K. Omri, L. Ei Mir, A. Houas, J Mater Sci: Mater Electron **27**, 8146 (2016).
[16] L. F. Koao, F. B. Dejene, M. Tsega, H. C. Swart, Physica B **480**, 53 (2016).
[17] J. K. Liang, H. L. Sua, C. L. Kuo, S. P. Kao, J. W. Cuia, Y. C. Wu, J. C. A. Huang, Electrochim. Acta **125**, 124 (2014).
[18] Y. Xu, B. Yao, Y. F. Li, Z. H. Ding, J. C. Li, H. Z. Wang, Z. Z. Zhang, L. G. Zhang, H. F. Zhao, D. Z. Shen, J. Alloys Compd. **585**, 479 (2014).

[19] H. L. Pang, X. H. Zhang, X. X. Zhong, B. Liu, X. G. Wei, Y. F. Kuang, J. H. Chen, J. Colloid. Interf. Sci. **319**, 193 (2008).
[20] P. V. Korake, A. N. Kadam, K. M. Garadkar, J. Rare Earths **32**, 306 (2014).
[21] J. Guo, J. Zheng, X. Z. Song, K. Sun, Mater. Lett. **97**, 34 (2013).
[22] T. V. L. Thejaswini, Deivasigamani Prabhakaran, M. Akhila Maheswari, J. Mater. Sci. **51**, 8187 (2016).
[23] M. Azarang, A. Shuhaimi, R. Yousefi, A. M. Golsheikh, M. Sookhakian, Ceram. Int. **40**, 10217 (2014).
[24] R. Ghomri, M. Nasiruzzaman Shaikh, M. I. Ahmed, M. Bououdina, M. Ghers, Appl. Phys. A **122**, 895 (2016).
[25] Y. F. Gomes, A. K. Freitas, R. M. Nascimento, M. R. D. Bomio, C. A. Paskocimas, F. V. Motta, J. Adv. Ceram. **5**, 103 (2016).
[26] V. Devi, M. Kumar, D. K. Shukla, R. J. Choudhary, D. M. Phase, R. Kumar, B. C. Joshi, Superlattice. Microst. **83**, 431 (2015).
[27] K. Vignesh, M. Rajarajan, A. Suganthi, J. Ind. Eng. Chem. **20**, 3826 (2014).
[28] M. R. Khodadad, M. E. Olya, A. Naeimi, Korean J. Chem. Eng. **33**, 2018 (2016).

* Corresponding author: jhzheng@chd.edu.cn